JOURNAL OF MATERIALS SCIENCE 29 (1994) 80–90

Effect of magnesium content and metal vanadate formation on the catalytic behaviour of $Cu_{1.0-x}$–Mg_x–$V_{2.0}$ oxide/vanadate ($0.0 \leq x \leq 1.0$) system

M. M. GIRGIS
Chemistry Department, Faculty of Science, Assiut University, Assiut, Egypt

The catalytic activity of the vapour-phase decomposition of 2-propanol over the $Cu_{1.0-x}$–Mg_x–$V_{2.0}$ oxide ($0.0 \leq x \leq 1.0$) series calcined between 500 and 1000 °C was investigated in the temperature range 165–375 °C using a flow system technique at atmospheric pressure. The catalysts were found to be selective dehydration types for 2-propanol. X-ray diffraction and scanning electron microscopy studies were used to identify the structural changes caused by the alcohol decomposition reaction. The activity and selectivity results were discussed on the basis of the electrical and/or acid–base properties of the catalysts, which not only depend on the sample composition, x, but also on its calcination temperature. A tentative reaction mechanism consistent with the obtained data has been suggested.

1. Introduction

In recent years, many workers have utilized mixed oxides [1, 2] and oxide solid solutions [1, 3] as model catalysts in an attempt to understand the mechanism of operation of such complex catalyst systems. Mixed vanadium pentoxide catalysts have been used effectively for numerous catalytic oxidation processes [1, 4–8]. Copper vanadates found applications in the oxidation of carbon monoxide [9] and the reduction of nitrous oxide [10]. The V–Mg–O system has been used for the conversion of ethylbenzene to styrene [11, 12] and butene to butadiene [13]. It also found application in the selective oxidative dehydrogenation of alkanes [1], propane [14] and butane [15].

One of the interesting mixed vanadium pentoxide systems is the $Cu_{1.0-x}$–Mg_x–$V_{2.0}$ oxide ($0.0 \leq x \leq 1.0$) series. This system shows drastic changes [16] in structure, grain morphology and electrical conductivity with increase in either the magnesium content or the calcination temperature. Therefore, it will be valuable to examine how these changes will affect the catalytic activity of these materials.

The decomposition of 2-propanol has gained a prominent place as a model for studying the principles of catalyst selection. In connection with our previous studies [2, 3, 17–19] in the field of catalysis, the present investigation was undertaken to follow up the catalytic behaviour of the two end members of the $Cu_{1.0-x}$–Mg_x–$V_{2.0}$ oxide series (i.e. at $x = 0.0$ and 1.0) calcined in the temperature range 500–1000 °C. Our investigation was extended to study the effect of the progressive increase in magnesium content ($0.1 \leq x \leq 0.9$) on the catalytic activity of these materials. Structural changes caused by the 2-propanol decomposition reaction were conducted using X-ray diffraction and scanning electron microscopy techniques.

2. Experimental procedure

2.1. Materials

All the reagents used in the present study were of analytical grade (BDH chemicals). The preparation of the catalysts under investigation was described previously [16]. Briefly, a series of $Cu_{1.0-x}$–Mg_x–$V_{2.0}$ mixed oxides (where $x = 0.0$, 0.1, 0.3, 0.5, 0.7, 0.9 and 1.0) were prepared by mixing ammonium metavanadate with CuO and/or MgO in the ratio of 2:1. The parent homogeneous mixtures were calcined in air for 5 h at 500, 700 and 1000 °C. The solids (500 °C samples) were slightly crushed to break up the crumbs, whereas the melts (700 and 1000 °C samples) were ground into fine powders after cooling and used as catalysts.

Analytical grade 2-propanol (BDH Ltd) was refluxed with sodium and distilled before use in catalytic runs. Its purity was verified by gas chromatographic analysis. Nitrogen was purified and dried as described elsewhere [18].

2.2. Characterization techniques for fresh and used catalysts

2.2.1. X-ray diffraction

The XRD patterns of the fresh and used catalysts were recorded using a Philips diffractometer (Model PW

0022–2461

1710) in the range of 2θ between 5° and 70°. A Philips generator operated at 40 kV and 30 mA provided a source of CuK_α radiation (nickel filtered). The phase identification was based upon the authentic patterns [20].

2.2.2. Scanning electron microscopy

Scanning electron micrographs were obtained using a Jeol JMS-T 200 scanning microscope (Jeol, Tokyo, Japan). Samples were prepared by the gold sputtering technique described previously [16].

2.3. Electrical conductivity measurements

The variation of the electrical conductivity occurring when the catalyst samples were exposed to 2-propanol vapour were measured at constant temperatures in the range 100–350 °C. The measurements were carried out with a conductivity cell described by Chapman *et al.* [21]. The temperature was controlled with a Digi-Sense temperature controller (Cole–Parmer Instrument Company, Chicago, IL). The resistance measurements were carried out using a 610 C Solid-State Electrometer (Keithley Instruments).

2.4. Catalytic activity and selectivity measurements

The catalytic activity was tested using the vapour-phase decomposition of 2-propanol in the temperature range 150–400 °C. The reactions were carried out in a fixed-bed flow-type integral reactor at atmospheric pressure. The exit feed was analysed by a direct sampling of the gaseous products (10 cm^3) into a Perkin Elmer gas chromatograph (Sigma 3 B). The flow system and technique have been described previously [18]. Purified dry nitrogen was used as a carrier gas in molar feed rate 3.5 mmol h^{-1}. 2-propanol vapour was charged at space velocity $W/F = 143.7\ g_{cat}\ h\ g^{-1}mol^{-1}$, where W is the weight of catalyst (0.5 g) and F is the molar feed rate (mol h^{-1}). All analytical measurements were made after the establishment of a steady activity level.

3. Results and discussion

3.1. Studies of structural changes during 2-propanol decomposition

The $Cu_{1.0-x}$–Mg_x–$V_{2.0}$ oxide (x = 0.0, 0.5 and 1.0) samples calcined at 500, 700 and 1000 °C for 5 h were investigated to trace structure modifications. X-ray diffraction patterns were recorded before and after 6 h use for 2-propanol decomposition at 350 °C in the flow method. Scanning electron micrographs were obtained for the samples before and after the reaction.

3.1.1. X-ray diffraction studies

X-ray analysis of the fresh and used $Cu_{1.0}$–$V_{2.0}$ oxide catalysts (Table I) indicates the appearance of Cu_2O (500 and 1000 °C) and Cu(1000 °C) in the course of 2-propanol decomposition reaction which reflects the reduction of copper (II) ions into lower valency states [22]. Also, the 700 and 1000 °C samples show remarkable structural changes during the decomposition process. On the other hand, the XRD patterns for the $Mg_{1.0}$–$V_{2.0}$ oxide catalysts show that the 500 °C primary oxides sample substantially changed to pyrovanadate structures after being used for 2-propanol decomposition, whilst those calcined at higher temperatures undergo either significant (700 °C sample) or non-significant (1000 °C sample) phase changes after the reaction (Table I). The patterns (Table I) indicate that the $Cu_{0.5}$–$Mg_{0.5}$–$V_{2.0}$ oxide catalysts undergo remarkable structural changes after the reaction, especially the 500 and 700 °C samples.

3.1.2. Grain-morphology examinations

Electron micrographs of the used $Cu_{1.0}$–$V_{2.0}$, $Mg_{1.0}$–$V_{2.0}$ and $Cu_{0.5}$–$Mg_{0.5}$–$V_{2.0}$ oxide catalysts calcined at 500–1000 °C are shown in Figs 1–3, respectively. Fig. 1a–c depict the morphology of the used $Cu_{1.0}$–$V_{2.0}$ oxide samples. Close examination of any particle in the 500 °C sample (Fig. 1a) indicated its irregular and porous nature. The grains of the 700 °C sample are mainly of elongated bars shape, Fig. 1b. Focusing the examination on one particle showed that the large faces have significant surface roughness. In this respect, the picture of the 1000 °C sample shows resemblance with that observed for the 700 °C one. The grain morphology of the used 500–1000 °C samples was somewhat similar to that of the fresh samples [16].

Fig. 2a shows that the used $Mg_{1.0}$–$V_{2.0}$ oxide sample calcined at 500 °C containing particles of less-uniform size and shape. Again, close examination of these particles confirmed that they were spongy and porous. It indicated also the presence of the fluffy [15] grains of MgO. The picture of the 700 °C sample (Fig. 2b) shows that it possessed poorly defined non-porous or slightly porous grains, whereas the picture of the 1000 °C sample (Fig. 2c) indicates that the grains are elongated bars of nearly rectangular section. The morphology of the used 500 and 700 °C samples was largely different from that of the corresponding fresh samples [16].

The grain morphology of the used $Cu_{0.5}$–$Mg_{0.5}$–$V_{2.0}$ oxide catalysts calcined at 500, 700 and 1000 °C are shown in Fig. 3a–c, respectively). This figure shows that the changes of the grain morphology characterizing the 700 and 1000 °C samples, with the calcination temperature, was somewhat similar to that of the corresponding used $Cu_{1.0}$–$V_{2.0}$ oxide samples. These changes were also somewhat similar to those of the fresh x = 0.5 samples [16] with much more significant surface roughness. The SEM examination results are in agreement with the XRD patterns of the catalysts taken after the reaction.

3.2. *In situ* measurement of electrical conductivity

The electrical conductivity changes occurring when a catalyst is exposed to 2-propanol vapour is indicative

TABLE I The characteristic phases present in the fresh and used $Cu_{1.0-x}$–Mg_x–$V_{2.0}$ oxide (x = 0.0, 0.5 and 1.0) catalysts calcined at different temperatures for 5 h

Catalyst	Calcination temp. (°C)[a]	Phase[b]								
		V_2O_5	CuO	Cu_2O	Cu	α-CuV_2O_6	B-$Cu_2V_2O_7$	α-$Cu_2V_2O_7$	$Cu_3V_2O_8$	Q
$Cu_{1.0}$–$V_{2.0}$	500 a	m	m	–	–	j	j	–	–	–
	b	m	m	m	–	j	j	–	–	–
	700 a	–	–	–	–	m	–	j	–	–
	b	–	–	–	–	–	–	j	–	j
	1000 a	–	–	–	–	–	–	j	m	–
	b	–	–	m	m	–	–	–	j	–
		V_2O_5		MgO		$Mg_2V_2O_7$		α-$Mg_2V_2O_7$	MgV_2O_6	$Mg(VO_3)_2$
$Mg_{1.0}$–$V_{2.0}$	500 a	j		j		–		–	–	–
	b	–		–		j		j	–	–
	700 a	–		–		–		–	j	–
	b	–		–		–		–	–	j
	1000 a	–		–		–		–	m	j
	b	–		–		–		–	m	j
		V_2O_5	MgO	α-CuV_2O_6	($Cu_{0.4}V_2O_5$) 44.4N	$Cu_3V_2O_8$	$Cu_4V_2O_9$	$Cu_2V_4O_{11}$	$Mg_2V_2O_7$	MgV_2O_6	$Mg_2V_6O_{17}$	$Mg(VO_3)_2$	Q
$Cu_{0.5}$–$Mg_{0.5}$	500 a	j	j	m	–	–	–	–	–	–	–	–	–
	b	–	–	–	j	j	j	–	j	–	–	–	–
	700 a	–	–	m	–	–	–	m	–	j	–	–	m
	b	–	–	–	–	–	–	–	–	j	j	–	j
	1000 a	–	–	–	–	–	–	–	–	m	–	–	j
	b	–	–	j	–	–	–	–	–	–	–	j	j

[a] a, Before the reaction; b, after 6 h use for 2-propanol decomposition at 350 °C.
[b] m, major; j, minor.

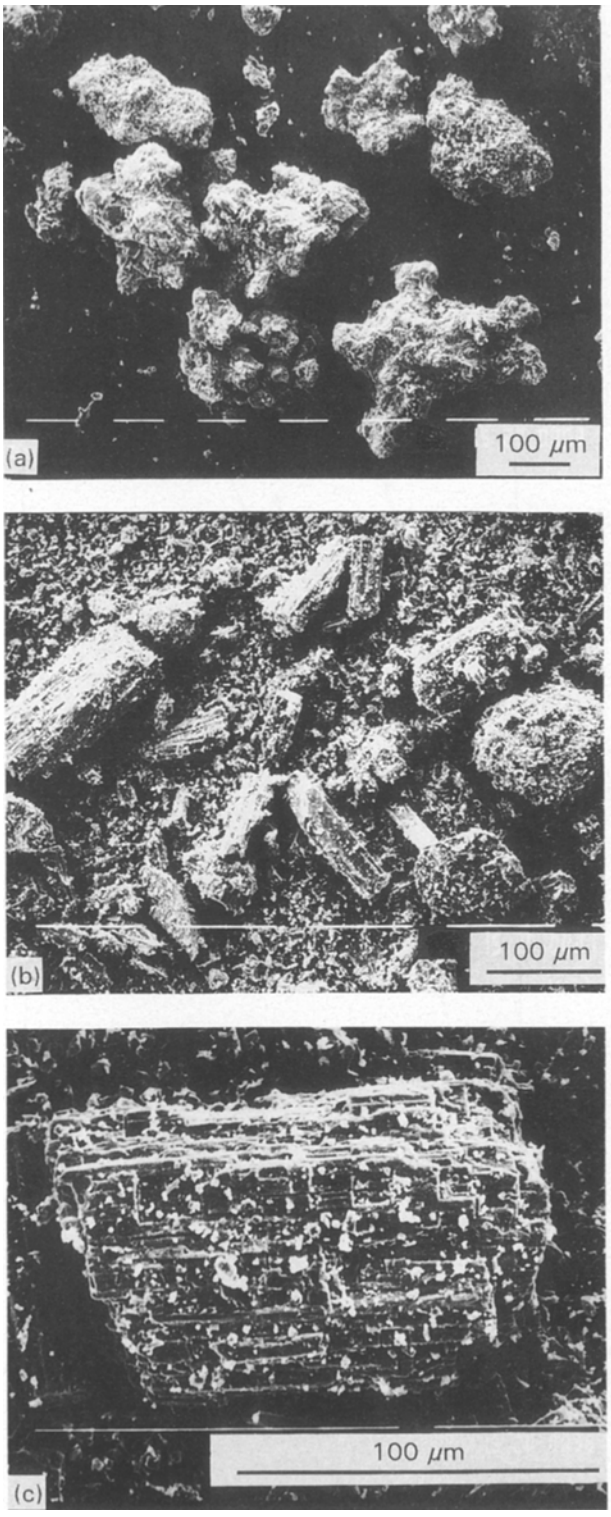

Figure 1 Scanning electron micrographs of the $Cu_{1.0}$–$V_{2.0}$ oxide system calcined at different temperatures for 5 h, after 6 h use for 2-propanol decomposition at 350 °C: (a) T_c = 500 °C, ×100; (b) T_c = 700 °C, ×200; and (c) T_c = 1000 °C, ×750.

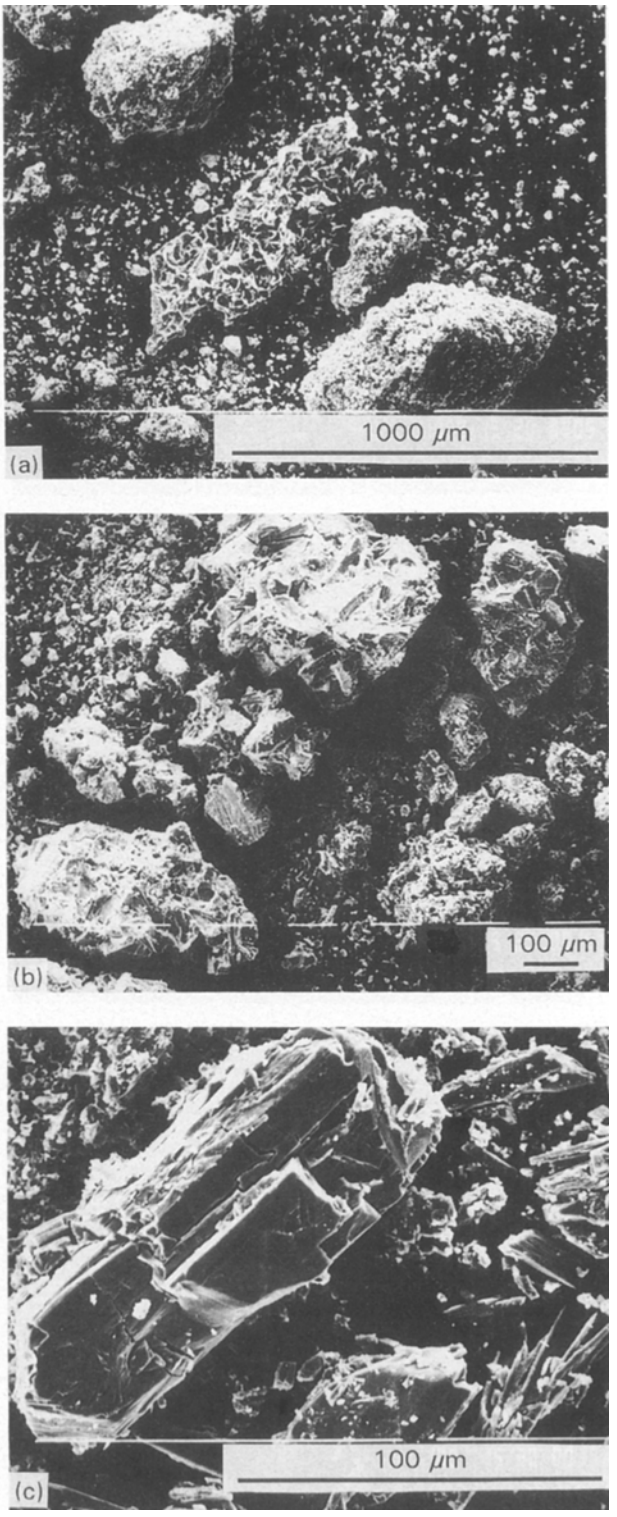

Figure 2 Scanning electron micrographs of $Mg_{1.0}$–$V_{2.0}$ oxide system calcined at different temperatures for 5 h, after 6 h use for 2-propanol decomposition at 350 °C: (a) T_c = 500 °C, ×75; (b) T_c = 700 °C, ×100; and (c) T_c = 1000 °C, ×750.

for electron transfer. *In situ* electrical conductivity measurements in ambient 2-propanol vapour atmosphere have been carried out on the catalyst samples at 100–350 °C. The conductivity data obtained at 350 °C for the $Cu_{1.0}$–$V_{2.0}$, $Cu_{0.5}$–$Mg_{0.5}$–$V_{2.0}$ and $Mg_{1.0}$–$V_{2.0}$ oxide samples calcined at 1000 °C and those obtained for the $Mg_{1.0}$–$V_{2.0}$ oxide sample calcined at 500, 700 and 1000 °C are represented in Fig. 4. The constant values of conductivity (obtained after ~ 60 min) can be attributed to the attainment of adsorption–desorption equilibrium. The increase in electrical conductivity caused by the admission of 2-propanol indicates that its adsorption is accompanied by donating electrons into the surface region of the catalyst.

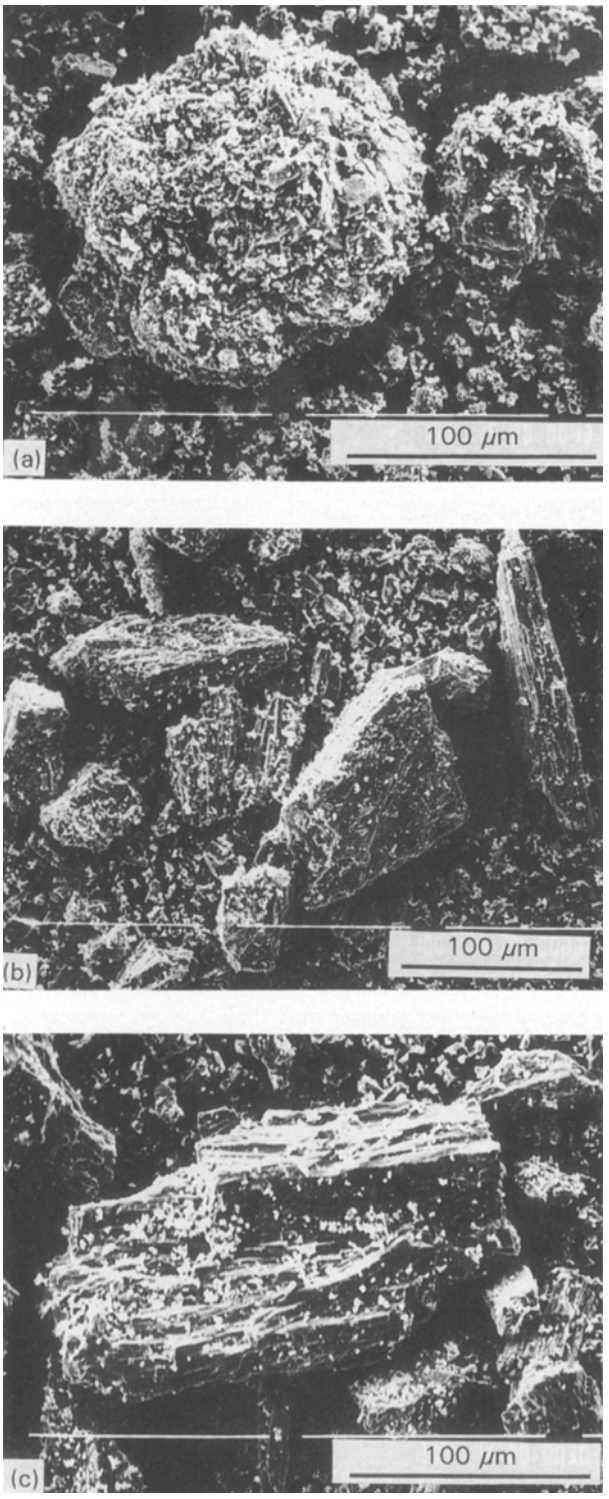

Figure 3 Scanning electron micrographs of $Cu_{0.5}$–$Mg_{0.5}$–$V_{2.0}$ oxide system calcined at different temperatures for 5 h, after 6 h use for 2-propanol decomposition at 350 °C:(a) T_c = 500 °C, ×500; (b) T_c = 700 °C, ×350; and (c) T_c = 1000 °C, ×500.

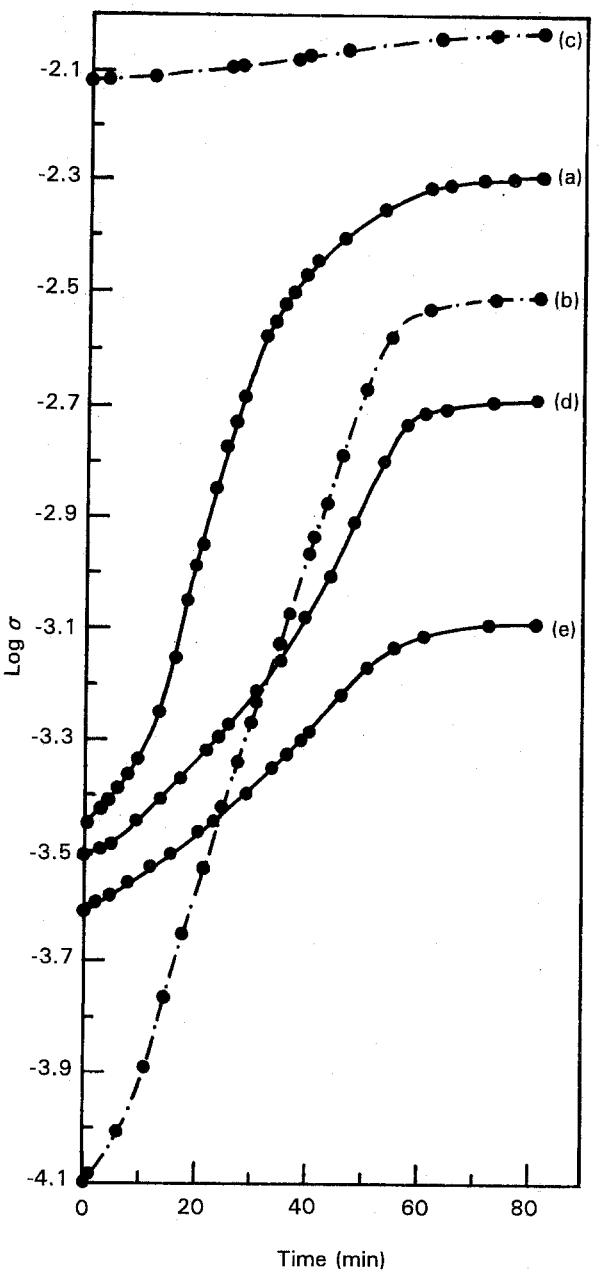

Figure 4 Variation of the electrical conductivity (log σ) values with time of 2-propanol admission at 350 °C for (a) $Cu_{1.0}$–$V_{2.0}$ oxide sample calcined at 1000 °C for 5 h; (b) $Mg_{1.0}$–$V_{2.0}$ oxide sample calcined at 1000 °C for 5 h; (c) $Cu_{0.5}$–$Mg_{0.5}$–$V_{2.0}$ oxide sample calcined at 1000 °C for 5 h; (d) $Mg_{1.0}$–$V_{2.0}$ oxide sample calcined at 500 °C for 5 h; (e) $Mg_{1.0}$–$V_{2.0}$ oxide sample calcined at 700 °C for 5 h.

3.3. Catalyst activity measurements

3.3.1. Effect of reaction temperature on the catalytic activity and dehydration selectivity of 2-propanol over $Cu_{1.0}$–$V_{2.0}$ and $Mg_{1.0}$–$V_{2.0}$ oxide catalysts

The effect of reaction temperature on the reaction products was studied firstly using the two end members, i.e. $Cu_{1.0}$–$V_{2.0}$ and $Mg_{1.0}$–$V_{2.0}$ oxide catalysts, calcined at 500, 700 and 1000 °C. The reaction temperature was raised to the selected temperature in a 150 ml min^{-1} (NTP) stream of nitrogen before admission of 2-propanol to the reactor. Experiments were carried out at various fixed temperatures ranging from 165–375 °C at a total flow rate of 5.8 $\times 10^{-5}$ mol min^{-1} (NTP). The steady state was attained after ~2 h. It was found that propylene is the main reaction product with a minor yield of acetone in the exit feed. The effect of reaction temperature on the per cent conversion, yields of propylene and acetone, and selectivities towards the dehydration and dehydrogenation pathways [18] over the 500, 700 and 1000 °C catalyst samples are represented in Figs 5 and 6.

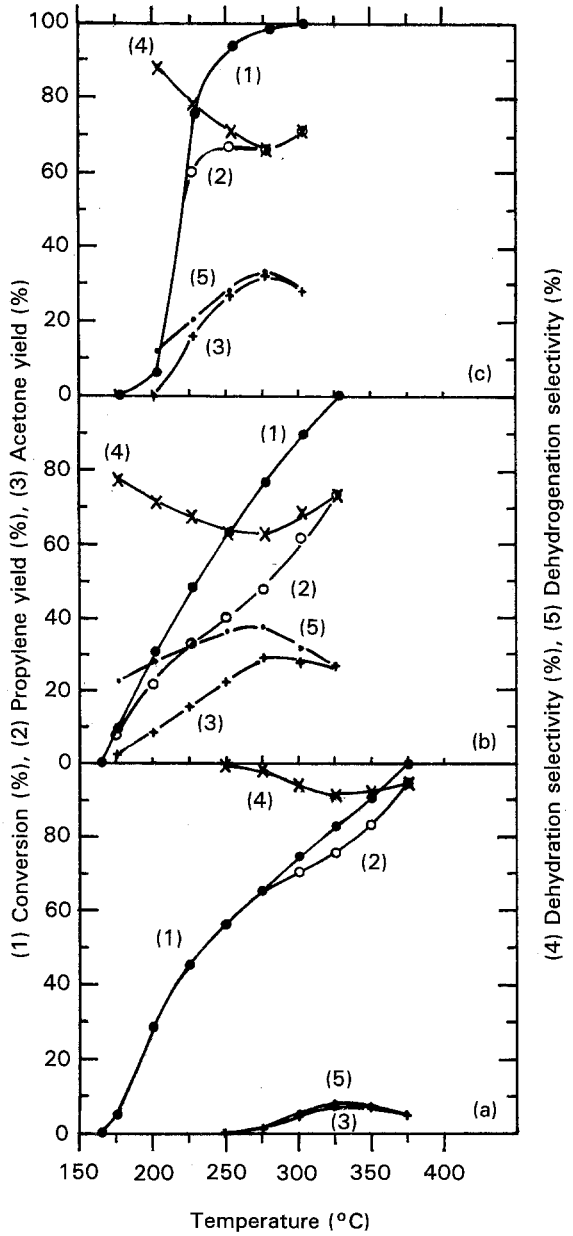

Figure 5 Variation of (1) per cent conversion, (2) yield of propylene or (3) acetone and (4) selectivity towards propylene or (5) acetone formation as a function of the reaction temperature for the $Cu_{1.0}$–$V_{2.0}$ oxide catalysts calcined at (a) 500 °C, (b) 700 °C and (c) 1000 °C for 5 h.

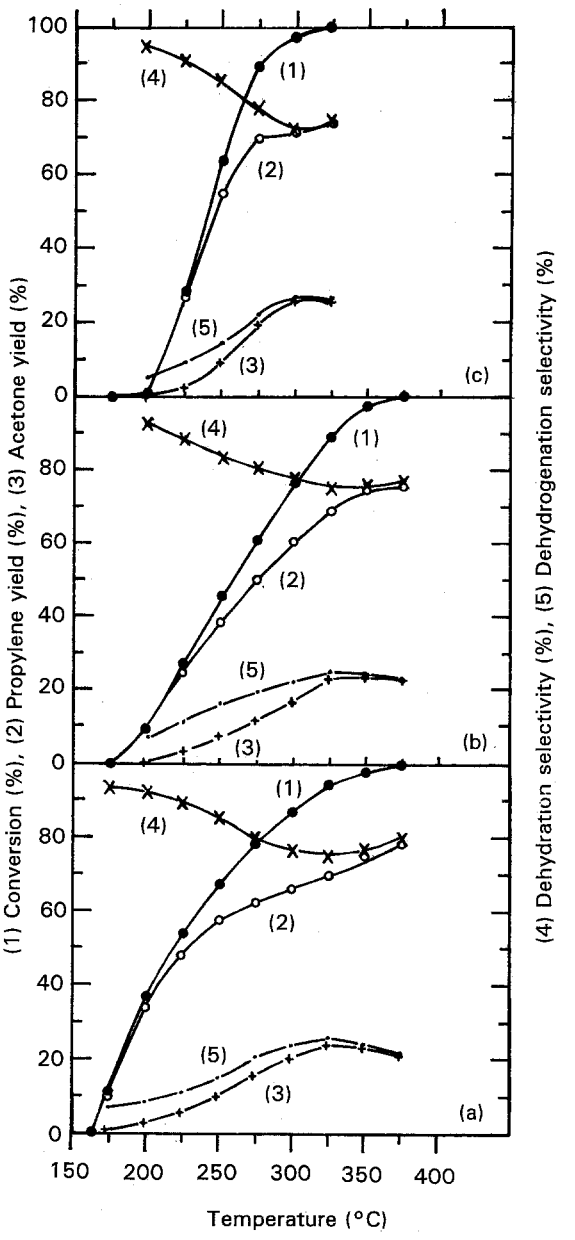

Figure 6 Variation of (1) per cent conversion, (2) yield of propylene or (3) acetone and (4) selectivity towards propylene or (5) acetone formation as a function of the reaction temperature for the $Mg_{1.0}$–$V_{2.0}$ oxide catalysts calcined at (a) 500 °C, (b) 700 °C and (c) 1000 °C for 5 h.

3.3.1.1. $Cu_{1.0}$–$V_{2.0}$ oxide catalysts. The activity and selectivity results (Fig. 5) can reflect the catalytic behaviour of the $Cu_{1.0}$–$V_{2.0}$ oxide samples as follows. The 500, 700 and 1000 °C catalysts are generally very active. As expected, an increase in the reaction temperature resulted in an increase in the per cent conversion. The conversion increases markedly, starting at ~175 °C, and reaching a maximum value (100%) ranging from 300–375 °C depending on the sample calcination temperature, T_c. Generally, the dehydration selectivity and yield of propylene show higher values compared to those of acetone. The yield of propylene and the selectivity towards its formation are higher for the 500 °C sample than for the 700 and 1000 °C ones. The propylene selectivity passed through a minimum where a maximum in acetone selectivity occurred.

Although an electronic mechanism involving the electrical properties of the semiconducting catalysts is generally postulated for 2-propanol dehydrogenation [23], the dehydration activity is believed to occur through a mechanism involving the acid centres localized on the surface of the catalyst [24]. The dehydration activity is adopted as a measure of the acidity [25]. Chakrabarty *et al.* [26] results showed just the opposite, where the involvement of acid centres could not successfully explain the alcohol dehydration process over the semiconducting oxide catalysts investigated [26]. The results of our study suggest that the dehydration activity of 2-propanol may also be explained in terms of their electrical properties. The relation between the electronic state of a catalyst and its catalytic activity is a consequence of the fact that the width of the energy gap and the position of the

Fermi level are important in controlling (i) the number of molecules which can be chemisorbed in the course of a catalytic reaction, and (ii) the nature of the chemical bond between the molecules and the surface [18, 27]. These factors simultaneously affect the activity and the mechanism of the catalytic reaction.

The catalytic activity of the $Cu_{1.0}$–$V_{2.0}$ oxide samples increases with increasing sample calcination temperature in the order: 500 °C < 700 °C < 1000 °C, where the conversion attained its maximum value (100%) at 350, 325 and 300 °C, respectively. According to Eucken and Hener [28] and Wicke [29], 2-propanol could be decomposed on a catalyst surface depending on the Fermi potential and the height of the potential barrier of the electrical field in the boundary layer which the electrons have to overcome during the exchange process. The electron which will move to the empty orbital will be the one with lower activation barrier to overcome. The activation energy required to move a bulk electron from one site to another will be given by the activation energy of polaron conduction [16]. Accordingly, the increase of activity with the rise of the catalyst calcination temperature, T_c, can be attributed to the decrease of the activation energy for electrical conduction, E_σ, with the increase of T_c, Table II. This parallelism between the decrease of activity with raising the activation energy barrier required by the bulk electrons to overcome provides a support for the concept that the catalytic reaction is controlled by electronic functions, where the ease with which an electron can be transported from the bulk seems to be of great importance in determining the extent of the adsorption process.

The higher dehydration selectivity of the 500 °C catalyst sample ($\geq$ 91.0%) relative to that of the 700 °C ($\geq$ 62.0%) or 1000 °C ($\geq$ 67.0%) sample (Fig. 5) can be explained in terms of the acid–base properties of these materials. In this respect the XRD studies (Table I) indicate that copper vanadates are the major phases present in the fresh and used 500, 700 and 1000 °C catalysts, whereas the primary metal oxides are present in appreciable amounts only in the 500 °C sample. It is well known that vanadium oxide is acidic in nature, whereas copper oxide, on the other hand, is basic [30]. Through the formation of copper vanadate much of the acid properties of V_2O_5 is removed [14]. Also, due to the higher electron density at the acetone carbonyl group relative to that at the propylene π bond, the acetone molecule is considered as more nucleophilic. Consequently, there is a much longer surface residence time for the produced acetone molecules on the acidic sites of the 500 °C catalyst surface relative to propylene molecules, and therefore propylene become the major and the higher decomposition product on this sample. In addition, the high selectivity towards acetone formation of the 1000 °C sample relative to the 500 °C one can be attributed to the reduction, during the 2-propanol decomposition process, of an appreciable amount of copper (II) ions into copper (Table I) which is a well-known dehydrogenation centre [31].

Furthermore, the high selectivity of the sample calcined at 500 °C towards propylene formation can be explained on the basis of the electrical conductivity behaviour in the following way. It is known that the hole defect structure enhances 2-propanol chemisorption [32], according to Equation 1

$$C_3H_7OH + |e|^{\bullet} \rightarrow C_3H_7OH^{+}_{ads} \qquad (1)$$

whereas water desorption is favoured by a surface having high electron concentration [26]. In addition, desorption of water seems to be the most likely rate-determining step [26], cf. mechanism. It follows that the dehydration selectivity is improved by the increase of the surface electron concentration. The latter is higher the larger the V^{4+} ion concentration, i.e. the higher the sample electrical conductivity, which depends on the ratio $[V^{4+}]/[V^{5+}]$ [16]. Inspection of the data in Table II shows that the electrical conduction of the 500 °C sample ($3.7 \times 10^{-4}\ \Omega^{-1}\ cm^{-1}$) is much higher than that of the corresponding 700 °C ($1.1 \times 10^{-4}\ \Omega^{-1}\ cm^{-1}$) or 1000 °C ($0.9 \times 10^{-4}\ \Omega^{-1}\ cm^{-1}$) catalyst samples and, consequently, the selectivity towards propylene formation is higher on the 500 °C sample relative to that on the 700 or 1000 °C sample.

3.3.1.2. $Mg_{1.0}$–$V_{2.0}$ oxide catalysts. The catalytic activity of the $Mg_{1.0}$–$V_{2.0}$ oxide samples increases with the catalyst calcination temperature in the order: 700 °C < 500 °C < 1000 °C, Fig. 6. The corresponding E_σ order is 500 °C $\gg$ 700 °C > 1000 °C, Table II. Therefore, the 500 °C catalyst shows a higher activity order than that expected on the basis of the conduction activation energy data. This can be attributed to

TABLE II Electrical conductivity, σ, at 300 °C, and activation energy, E_σ data [22] for the $Cu_{1.0-x}$–Mg_x–$V_{2.0}$ oxide ($0.0 \leq x \leq 1.0$) system calcined at 500, 700 and 1000 °C

x	500 °C		700 °C		1000 °C	
	$\sigma(10^5\ \Omega^{-1}\ cm^{-1})$	$E_\sigma(10^2$ eV)	$\sigma(10^5\ \Omega^{-1}\ cm^{-1})$	$E_\sigma(10^2$ eV)	$\sigma(10^5\ \Omega^{-1}\ cm^{-1})$	$E_\sigma(10^2$ eV)
0	37.068	13.54	11.220	12.92	8.710	8.74
0.1	63.196	12.31	38.905	11.95	16.218	8.60
0.3	5.888	13.79	10.000	9.93	4.467	8.20
0.5	1.549	14.36	562.341	8.25	154.882	7.60
0.7	5.012	11.27	12.589	10.57	7.499	10.10
0.9	0.501	14.10	2.570	13.65	5.012	13.20
1.0	0.001	28.73	1.259	14.75	2.985	14.15

the intimate presence of both vanadium and magnesium oxides in the fresh 500 °C sample, Table I. In this sample, the role of MgO is to induce the preferential formation of a particular surface-exposed plane of V_2O_5 on MgO substrate [33, 34]. Vanadium oxide possesses a terminal V=O group characterized [16] by an infrared stretching frequency at 1000 cm^{-1}. As shown previously [16], the surface density of V=O is higher on the 500 °C than on the 700 °C sample. However, there is no V=O on the 1000 °C sample. Therefore, the 500 °C sample is more active, because the terminal adjacent V=O groups were identified by various techniques as the active surface sites [33, 35–37]. Also, MgO is believed to increase the reactivity of the V=O group by weakening its strength [6] on the exposed V_2O_5 plane [33, 34]. This finding was supported by the analysis of the XRD pattern of the used catalyst where a transformation to the pyrovanadate structure occurred (Table I).

The effect of 2-propanol on log σ for these $Mg_{1.0}$–$V_{2.0}$ oxide catalysts supported the results of catalytic activity measurement, where the electrical conductivity changes for the 500 °C sample are more pronounced than those for the 700 °C one. The conductivity change increases in the T_c order: 700 °C < 500 °C < 1000 °C (Fig. 4) which is consistent with the observed catalytic activity order of these samples.

3.3.2. Effect of catalyst composition, x, on the catalytic activity and dehydration selectivity of 2-propanol over $Cu_{1.0-x}$–Mg_x–$V_{2.0}$ oxide system

The effect of magnesium content, x, on the catalytic properties of $Cu_{1.0-x}Mg_x$–$V_{2.0}$ oxide (x = 0.0, 0.1, 0.3, 0.5, 0.7, 0.9 and 1.0) series calcined at 500 and 700 °C was investigated at a selected constant reaction temperature (300 °C). The values of the overall 2-propanol conversion, propylene yield and dehydration selectivity are plotted with respect to catalyst composition, x, in Figs 7 and 8. These results show a strong dependence of the catalytic activity and dehydration selectivity on the composition of the catalyst which, in turn, is largely influenced by the catalyst calcination temperature.

For the 500 °C samples, the conversion (Fig. 7a) increases from 74.4% at x = 0.0 passing through a maximum value (100%) at x = 0.5, then gradually decreases down to 86.6% at x = 1.0. The 700 °C samples show a similar trend with a broad maximum (100%) at x between 0.5 and 0.6. The 700 °C samples were superior to the 500 °C ones at $x \leq 0.7$. This high activity of the 700 °C samples ($x \leq 0.7$) relative to the 500 °C ones may be attributed again to the weakening of the V=O bond strength and consequently the increase of its reactivity with raising the catalyst calcination temperature [38, 39], whereas the high activity of the 500 °C samples at $x \geq 0.9$ can be correlated to the increase in the surface concentration of the V=O species on these samples.

The effect of catalyst composition on the yield of propylene (Fig. 7b) over the 500 °C samples shows

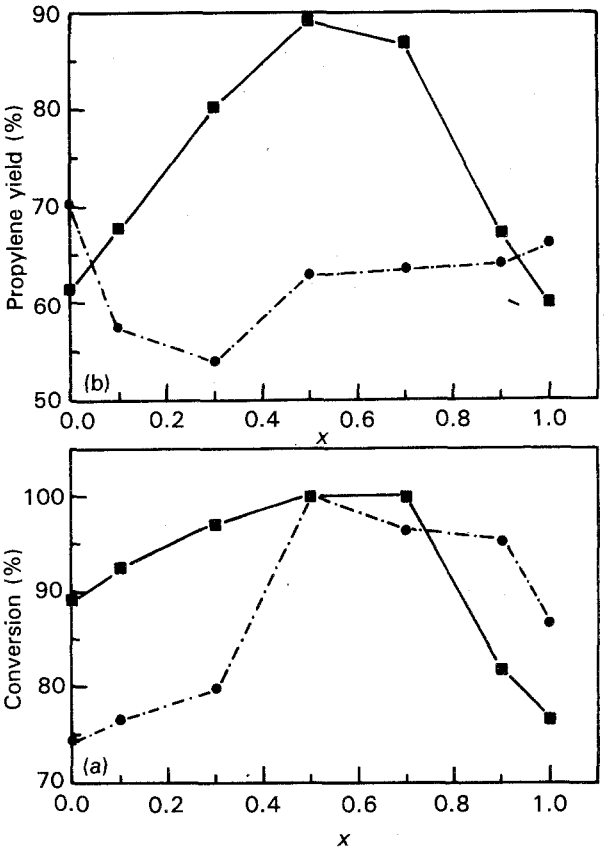

Figure 7 Variation of (a) per cent conversion, (b) propylene yield as a function of the catalyst composition, x, for the $Cu_{1.0-x}$–Mg_x–$V_{2.0}$ oxide series calcined at (●) 500 °C and (■) 700 °C for 5 h.

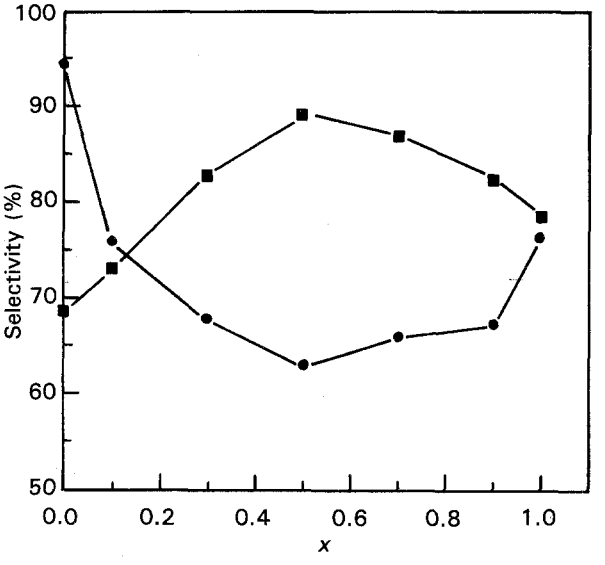

Figure 8 Variation of dehydration selectivity percentage as a function of the catalyst composition, x, for the $Cu_{1.0-x}$–Mg_x–$V_{2.0}$ oxide series calcined at (●) 500 °C and (■) 700 °C for 5 h.

that the yield decreases markedly from 70.2% at x = 0.0, passing through a minimum value (54.1%) at x = 0.3, then gradually increases up to 66.1% at x = 1.0. The 700 °C catalyst samples show another trend, where the yield of propylene passes through a maximum at x = 0.5. Also, the 700 °C catalyst samples were superior to the 500 °C ones in the composition range $0.1 \leq x \leq 0.9$. These catalytic activity results

(Fig. 7b) can be interpreted as follows. In the 500 °C samples, the composition $x = 1.0$ represents the primary oxides with a layer structure of V_2O_5 on an MgO substrate [33, 34]. This 500 °C sample is active, because the terminal-weakened [39] V=O groups are active sites for 2-propanol decomposition [36, 37]. The decrease in activity on raising the copper content up to $x = 0.7$ can be attributed to the solid-state reaction with gradual formation of copper vanadates [16], which reduces the vanadium oxide content and consequently the active V=O sites. The intensity of the V=O stretching frequency is more pronounced in the fresh 500 °C $Mg_{1.0}$–$V_{2.0}$ oxide sample than in the corresponding $Cu_{0.5}$–$Mg_{0.5}$–$V_{2.0}$ oxide sample [16], which supports our catalytic results. On the other hand, the yield of propylene decreases from 70.2% on the 500 °C $Cu_{1.0}$–$V_{2.0}$ oxide sample (i.e. at $x = 0.0$) to 57.5% and 54.1% on increasing the magnesium content, x, in the order 0.0, 0.1 and 0.3, respectively. This can be attributed to the gradual increase of the bond energy of the surface oxygen in the same order [40], because the O–Cu bond strength (82 $\pm$ 15 kcal mol^{-1}) [41] is lower than that of O–Mg (94.1 $\pm$ 8.4 kcal mol^{-1}) [41]. The samples prepared at 700 °C are the metal vanadates produced by quenching the melts to room temperature. The catalytic activity towards propylene production increases with the increase of the sample magnesium content up to 0.5, then decreases up to $x = 1.0$. This can be attributed to the decrease of E_σ in the same order up to $x = 0.5$, followed by an increase up to 1.0, Table II. This provides further support to the concept that the catalytic reaction is controlled by electronic func.

The effect of catalyst composition, x, on the dehydration selectivity is illustrated in Fig. 8. For the 500 °C catalyst samples, the selectivity decreases from 94.5% on the $Cu_{1.0}$–$V_{2.0}$ oxide sample ($x = 0.0$) to 76.0%, 68.0% and 63.0% by increasing the sample magnesium content in the order 0.1, 0.3 and 0.5, respectively. This can be correlated with the interaction between MgO and V_2O_5 according to the mechanism

$$2MgO = 2Mg|V|''' + V_2O_5 + 3|O|^{2-} \quad (2)$$

where $Mg|V|'''$ is the Mg^{2+} ion replacing the V^{5+} ion in its normal lattice site and $|O|^{2-}$ is a lattice oxygen deficiency. The surface is now active in producing acetone, at the expense of propylene formation, because effective charge delocalization, which is responsible for the dehydrogenation process, can be accomplished by the oxygen vacancies produced on the surface. In addition, the decrease of the dehydration selectivity with increasing x in the order $0.1 > 0.3 > 0.5$ can also be explained in terms of the decrease of the electrical conductivity, and consequently the surface electron concentration, in the same order, Table II.

On the other hand, the selectivity towards propylene formation decreases from 76.4% on the $Mg_{1.0}$–$V_{2.0}$ oxide catalyst ($x = 1.0$) to 67.3%, 66.0% and 63.0% by the gradual increase of the sample copper content in the (x) order 0.9, 0.7 and 0.5, respectively. In these 500 °C catalysts, the surface of the $x = 1.0$ sample is acidic. The decrease in the dehydration selectivity on raising the copper content up to $x = 0.5$ can be attributed to the gradual reduction of the surface acidity of the catalyst, i.e. the decrease of the number of acidic sites conducive to dehydration. The selectivity towards propylene formation is higher for the 700 °C samples (at $x > 0.1$) relative to that for the corresponding 500 °C ones with a maximum value at $x = 0.5$. Inspection of the conductivity data given in Table II shows that the electron conduction of these 700 °C samples (at $x > 0.1$) is higher than that of the corresponding 500 °C ones with a maximum value at $x = 0.5$ and accordingly the selectivity has the same trend. The selectivity of the 700 °C catalysts at $x \leq 0.1$ is lower than that of the 500 °C ones. This can be correlated to the electronic as well as the acidic properties of these samples as described above.

3.4. Reaction mechanism

Two general models have been used in interpreting the activity results: "the rigid band model" in which surface electronic states provide the possibility of electron transfer through semiconductivity [42–44] and the surface molecule model in which the catalyst activity is assumed to reside in specific sites [45–47]. We have preferred a catalytic mechanism intermediate between these two extremes, whereby localized adsorption occurs on specific coordinatively unsaturated sites, but electron availability occurs through electron-exchange interaction with nearby metal ions.

Hauffe [27] and Wolkenstein [48] have regarded a catalyst as a non-structured solid phase with semiconducting properties which govern the mechanism and the activity of the catalyst. Reactant and product inhibition studies were carried out on some vanadium oxide systems [26]. Chakrabarty *et al.*'s [26] results showed that the dehydration rates are independent of either the partial pressure of 2-propanol or propylene but they decrease rapidly on increasing the partial pressure of water vapour. These findings indicate that the desorption of propylene is a fast process and refer to its poor competition for the surface. At the same time, the rate of desorption of water must be slower and it can be considered as the most likely rate-determining step [26].

The increase in conductivity caused by the admission of 2-propanol is attributed to the transfer of electrons from the oxygen of the alcohol to the catalyst surface during the process of adsorption and lends a support to the n-type nature of these materials [3]. Sedláček and Kraus [49] reported that this adsorption process on an electron acceptable centre (i.e. an acidic site) leads to the dehydration process. The presence of a basic site adjacent to an acidic site is conducive to alcohol dehydration [50, 51]. The surface vanadium–oxygen centres were identified by various techniques as the active surface sites [36, 37]. These acidic sites serve to activate electron-donating (basic) alcohol molecules by means of acid–base type interaction. In addition the hole defect structure enhances 2-propanol chemisorption [32]. This adsorbed

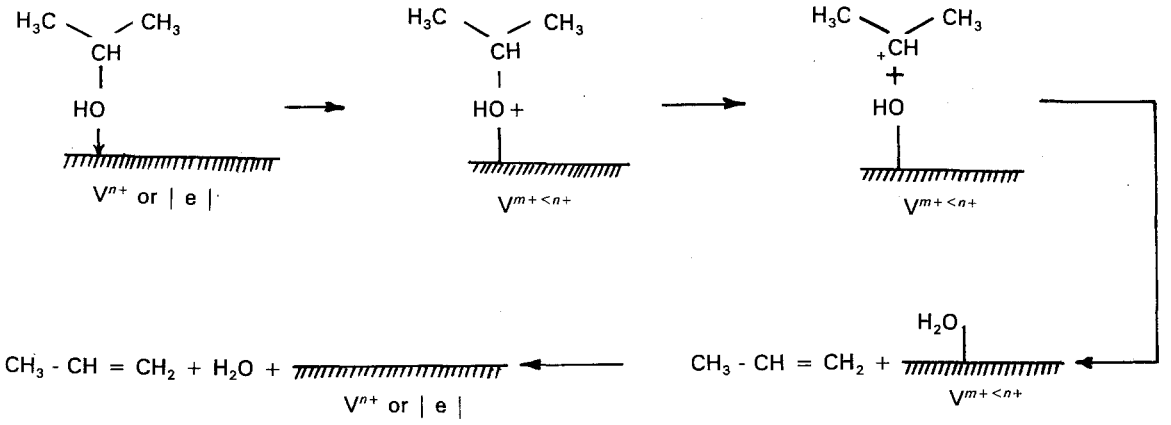

Scheme I

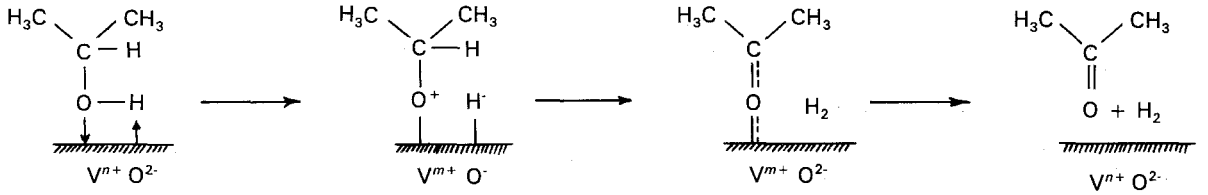

Scheme II

positively charged alcohol molecule represents a site for recombination of an electron coming from the forbidden band. Accordingly, and based on the available data, one can suggest the dehydration reaction of 2-propanol to proceed according to Scheme I [3] as follows: (i) 2-propanol molecule is adsorbed via the unpaired electrons of its hydroxyl oxygen on a surface active site (V^{n+})/or a positive hole $|e|^{\bullet}$; simultaneously the C–OH bond becomes weaker [52]; (ii) the C–OH bond is ruptured, leaving the alcohol molecule as a carbonium ion, and the hydroxyl group becomes bound to the active centre/or the hole. The active site is partially reduced while the hole is destroyed as a consequence of the approach of the oxygen lone pair electrons [53]; (iii) carbonium ion rearrangement results in the formation of propylene and the released hydrogen ion reacts with the hydroxyl group to form an H_2O molecule, which (iv) is desorbed.

On the other hand, the presence of acetone as a minor product in the decomposition process can be visualized as a result of another type of surface reaction, taking place on active centres formed by pairs of V^{n+} and O^{2-} ions [18, 54]. Considering the different models proposed [54–56] for the catalytic dehydrogenation of alcohols, the mechanism given in Scheme II can be proposed.

References

1. D. K. PATEL, Avail. Univ. Microfilms. Int., Order DA 8902685, from *Diss. Abstr. Int. B* **49** (1989) 4930.
2. M. M. GIRGIS, R. M. GABR and A. M. EL-AWAD, *Croat. Chem. Acta* **64** (1991) 207.
3. R. M. GABR, A. M. EL-AWAD and M. M. GIRGIS, *J. Mater. Chem. Phys.* **30** (1991) 69.
4. A. ZYCHIEWICZ (Akademia Ekonomiczna, Wroclaw) Pol. PL. Pat. 138258, 31 March 1987; *Chem. Abstr.* **110** (1989) 10935 n.
5. H. P. ANGSTADT (Suntch, Inc.) Can. pat. 1072580, 26 February 1980; *Chem. Abstr.* **93** (1980) 95023 s.
6. I. V. SHAKIROV, YU. S. CHEKRYSHKIN and V. I. ABANIN, *Kinet. Katal.* **26** (1985) 356.
7. G. W. YOUNG and H. L. GREENE, *J. Catal.* **50** (1977) 258.
8. D. J. COLE, C. F. CULLIS and D. J. HUCKNALL, *J. Chem. Soc. Faraday Trans. 1.* **72** (1976) 2744.
9. S. YOSHIDA, A. UEDA and K. TARAMA, "Studies in Surface Science and Catalysis 7B. New Horizons in Catalysis" Part B edited by T. Seiyama and K. Tanabe (Elsevier Scientific, Amsterdam, 1981) p. 1377.
10. S. YOSHIDA, A. UEDA and K. TARAMA, *Ind. Eng. Chem. Prod. Res. Dev.* **18** (1979) 283.
11. W. OGANOWSKI, A. NOWICKI and J. HANUZA, *Bull. Pol. Acad. Sci. Chem.* **31** (1984) 129.
12. J. HANUZA, B. JEZOWSKA-TRYEBRATOWSKA and W. OGANOWSKI, *J. Mol. Catal.* **29** (1985) 109.
13. A. V. SIMAKOV and S. A. VENIAMINOV, *React. Kinet. Catal. Lett.* **28** (1985) 67.
14. M. A. CHAAR, D. PATEL and H. H. KUNG, *J. Catal.* **109** (1988) 463.
15. M. A. CHAAR, D. PATEL. M. C. KUNG and H. H. KUNG, *ibid.* **105** (1987) 483.
16. M. M. GIRGIS, *J. Mater. Sci.* (1992) in press.
17. R. M. GABR, M. M. GIRGIS and A. M. EL-AWAD, *Langmuir* **7** (1991) 1642.
18. R. M. GABR, M. M. GIRGIS, and A. M. EL-AWAD, *J. Mater. Chem. Phys.* **28** (1991) 413.
19. M. M. GIRGIS and A. M. EL-AWAD, *J. Mater. Chem. Phys.*, **36** (1993) 48.
20. W. F. McCLUNE (ed.), "Powder Diffraction File (Inorganic Phases)" (JCPDS International Centre for Diffraction Data, Philadelphia USA, 1984).
21. P. R. CHAPMAN, R. H. GRIFFITH and J. D. F MARSH, *Proc. R. Soc. Lond.* **224** (1954) 419.
22. J. C. VOLTA, P. TURLIER and Y. TRAMBOUZE, *J. Catal* **34** (1974) 329.
23. O. V. KRYLOV, *Zh. Fiz. Khim.* **39** (1965) 2911.
24. *Idem, ibid.* **39** (1965) 2656.
25. M. AI, *J. Catal.* **54** (1978) 426.
26. D. K. CHAKRABARTY, D. GUHA, I. K. BHATNAGAR and A. B. BISWAS, *ibid.* **45** (1976) 305.
27. K. HAUFFE, *Adv. Catal.* **7** (1955) 213.
28. A. EUCKEN, and K. HENER, *Z. Phys. Chem.* **169** (1950) 40.

29. E. WICKE, *Z. Electrochem.* **52** (1948) 86.
30. M. AI, *J. Syn. Org. Chem. Jpn* **35** (1977) 201.
31. P. W. SELWOOD and N. S. DALLAS, *J. Am. Chem. Soc.* **70** (1948) 2145.
32. K. M. ABD EL-SALAAM and A. A. SAID, *Surf. Technol.* **17** (1982) 199.
33. A. MIYAMOTO, Y. YAMAZAKI, M. INOMATA and Y. MURAKAMI, *J. Phys. Chem.* **85** (1981) 2366.
34. M. INOMATA, A. MIYAMOTO and Y. MURAKAMI, *ibid.*, **85** (1981) 2372.
35. M. INOMATA, A. MIYAMOTO and Y. MURAKAMI, *J. Catal.* **62** (1980) 140.
36. F. J. J. G. JANSEN, F. M. G. KERHOFF, H. BOSCH and J. R. H. ROSS, *J. Phys. Chem.* **91** (1987) 5921.
37. Y. NAKAGAWA, T. ONO, H. MIYATA and Y. KUBOKAWA, *J. Chem. Soc. Faraday Trans. 1* **79** (1983) 2929.
38. K. TARAMA, S. YOSHIDA, S. ISHIDA and H. KAKIOKA, *Bull. Chem. Soc. Jpn* **41** (1968) 2840.
39. K. TARAMA, S. TERANISHI, S. YOSHIDA and N. TAMURA, in "Proceedings of the 3rd International Congress on Catalysis", Vol. 1 (North-Holland, Amsterdam, 1965) p. 282.
40. M. NAKAMURA, K. KAWAI and Y. FUJIWARA, *J. Catal.* **34** (1974) 345.
41. R. C. WEAST and M. J. ASTLE, "CRC Handbook of Chemistry and Physics", 61st Edn. (1980–1981) (CRC Press Inc., Boco Raton, Florida, USA) p. F-220.
42. J. C. KURIACOSE and C. DANIEL, *J. Catal.* **14** (1969) 77.
43. S. R. MORRISON, *ibid.* **47** (1977) 69.
44. S. R. MORRISON, *Chemtech.* **7** (1977) 570.
45. L. NONDEK and M. KRAUS, *J. Catal.* **40** (1975) 40.
46. L. NONDEK, D. MIHAJLOVA, A. ANDREAV, A. PALAZOV, M. KRAUS and D. SHOPOV, *ibid.* **40** (1975) 46.
47. A. A. DAVYDOV, YU. M. SHCHEKOCHIKHIN and N. P. KEIER, *Kinet. Katal.* **13** (1972) 1088.
48. T. WOLKENSTEIN, "Advances in Catalysis", Vol. XII (Academic Press, New York, 1960) p. 189.
49. J. SEDLÁČEK and M. KRAUS, *React. Kinet. Catal. Lett.* **2** (1975) 27.
50. F. FIGUERAS, A. NOHL, L. DEMOURGES and Y. TRAUMBOUZE, *Trans. Faraday Soc.* **67** (1971) 1155.
51. K. R. BAKSHI and G. R. GAVALAS, *J. Catal.* **38** (1975) 312.
52. A. M. EL-AWAD and K. M. ABD EL-SALAAM, *Monatsh. Chem.* **119** (1988) 1057.
53. E. I. ODUMAH and J. C. VICKERMAN, *J. Catal.* **62** (1980) 195.
54. L. NONDEK and J. SEDLACEK, *ibid.* **40** (1975) 34.
55. K. BALASUBRAMANIAN and J. C. KURIACOSE, in "Proceedings of the 8th International Congress on Catalysis", Berlin, Germany, 1984, Vol. IV, p. 623.
56. J. C. KURIACOSE, C. DANIEL and N. BALAKRISHNAN, *Indian J. Chem.* **7A** (1969) 367.

Received 19 June 1992
and accepted 20 April 1993